

Density Functional Study of Structural and Electronic Properties of Small Bimetallic Silver–Nickel Clusters

M. Harb, F. Rabilloud,* and D. Simon

Université Lyon 1, CNRS, LASIM UMR 5579, bât A. Kastler, 43 boulevard du 11 novembre 1918, F-69622 Villeurbanne, France

Received: March 20, 2007; In Final Form: May 28, 2007

Theoretical study on the structure and electronic properties of small Ag_mNi_p ($m + p \leq 6$) clusters has been carried out in the framework of density functional theory. Structural features, cohesive energies, vertical ionization potentials, and charge transfers are evaluated for each Ag/Ni ratio. In all the Ag_mNi_p clusters, the nickel atoms are brought together, yielding a maximum of Ni–Ni bonds, and the silver atoms are located around a Ni core with a maximum of Ag–Ni bonds. The ionization potential and the highest occupied molecular orbital shape are directly related to the two- or three-dimensional character of the cluster's geometry. A very low electronic charge transfer from Ni to Ag is found, and the magnetic moment is located on Ni atoms but with a low spin polarization on silver in the Ni-rich clusters.

1. Introduction

Bimetallic nanoclusters have received considerable attention recently¹ for their particular and unique structural,^{2–7} electronic,^{2,3} optical,^{8–10} and magnetic^{11–13} properties and their importance in catalysis^{14,15} and nanotechnology. The reason for the increasing interest in bimetallic clusters is that their properties depend not only on the size but also on the chemical composition and the atomic arrangement. This leads to a large variety of applications: there is technological interest in developing new nanodevices for electronics,¹⁶ and for optics, the bimetallic clusters could play an important role in the enhancement of nonlinear optical properties over the bulk metals.¹⁷

In the nanoscale, bimetallic clusters are found either as random alloys or as segregated structures. This depends mainly on the nature of the two metal components but also on the method of preparation.¹⁰ Nevertheless, for clusters of a few hundreds of atoms where quantum size effects are important, there are very few experimental studies. From the theoretical point of view, the starting point for the study of gas-phase nanoalloy cluster properties is the determination of their most favorable structures, depending on size and composition. Presently, the determination of the most stable geometrical structure of the bimetallic clusters remains a challenge due to the huge amount of combinatorial possibilities of isomers. If one metal is magnetic, the study becomes more complicated because several spin states must be investigated.

It has been shown previously^{4–7,10} that large Ag–Ni bimetallic particles adopt a core–shell configuration with a Ni core and external Ag atoms. Several families of AgNi polyicosahedral structures of bimetallic clusters have been described by a semiempirical global optimization method^{4–6} and by density functional theory (DFT)^{4,7} and have been shown to give rise to “magic” clusters, that is, clusters of remarkable structural, electronic, and thermodynamic stability with a low fraction of Ni occupying the inner and outer Ag atoms in a core–shell

atomic arrangement. In recent optical properties determination combined with theoretical calculations,¹⁰ it has been shown, by comparing the experimental results with a core model surrounded by a size-dependent damping constant silver shell, that Ag–Ni nanoclusters adopt a Ni core–Ag shell configuration.

High-level quantum calculations cannot be performed on large clusters. Nevertheless, the theoretical investigation of properties of very small clusters (with less than 10 atoms) may give valuable information on the general behavior of bimetallic particles. For example, a recent work¹⁸ has used DFT to investigate the low-lying electronic states of neutral and anionic Ni-doped $\text{Ag}_5\text{Ni}^{0,-}$ clusters. Planar and three-dimensional structures have been discussed, and for the neutral Ag_5Ni cluster the most stable structure is pentagonal with a core Ni atom.

In this paper, we investigate the tendency of AgNi clusters to form a core–shell structure in the case of small clusters. Many structures have been studied with DFT calculations, leading to a large range of geometrical and configurational possibilities. Moreover, the small size enables an analysis of the energetic properties in relationship to the electronic structure of the clusters. We present a systematic study of the geometrical structures of the bimetallic nanoclusters Ag_mNi_p ($m + p \leq 6$), compared to Ag_m and Ni_p . The study of the modulation of their electronic properties [vertical ionization potential, cohesive energy, and highest occupied molecular orbital (HOMO)] as a function of the size and chemical composition is performed by density functional theory (DFT), which is nowadays one of the best methods to study small and medium-size systems.

2. Computational Methods

We have used the DFT technique implemented in Gaussian 98,¹⁹ combined with relativistic effective core potentials (RECP) to optimize the geometry of several configurations of bimetallic Ag_mNi_p ($m + p \leq 6$) clusters. We have used the exchange and correlation functional of second generation of type GGA (generalized gradient approximation) called BP86, which includes the exchange functional of Becke²⁰ and the correlation functional of Perdew.²¹ Previous studies on the structural,

* Corresponding author: tel 33 4 72 43 29 31; fax 33 4 72 43 15 07; e-mail franck.rabilloud@lasim.univ-lyon1.fr.

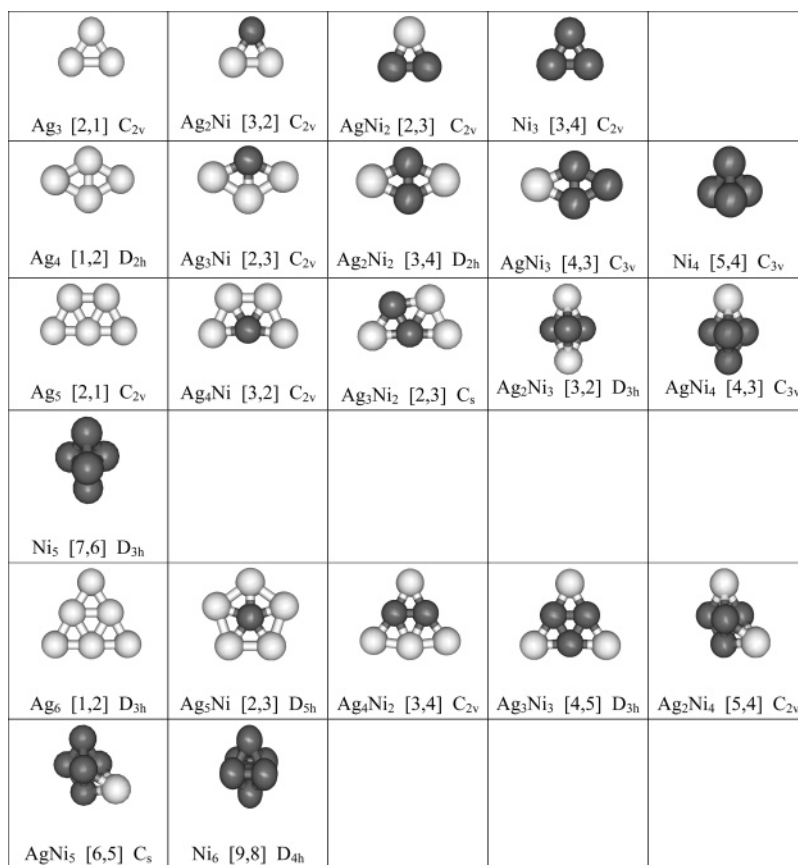


Figure 1. Optimized geometries of the lowest-energy isomers for Ag_mNi_p clusters with $m, p \leq 6$. The spin multiplicities of neutral (first entry) and cationic (second entry) systems are given in brackets, and spatial symmetries are also given.

electronic, and optical properties of the silver clusters or binary clusters including Ag atoms have shown that explicit treatment of the 4s, 4p, and 4d electrons of silver atoms like active valence electrons are necessary to describe in a correct way the electronic structure.^{22–26} Following this, the LANL2DZ RECP,²⁷ which replace 28 electrons on Ag atoms and 18 electrons on Ni atoms, were used. The associated Gaussian basis sets were (8s5p5d) contracted in [3s3p2d] on nickel atoms, and (8s6p4d) contracted in [3s3p2d] on silver atoms as displayed in Gaussian98. Calculations have been performed with the graphical user interface Gabedit.²⁸

In the optimization process of cluster geometries, a number of structures were tested for each size. We have initiated the geometry optimization process of Ag_mNi_p clusters from the known frame of the corresponding two-dimensional Ag_m clusters in which some Ag atoms were replaced by Ni atoms. We have tested three-dimensional structures like those of Ni_p. We have also tested structures for which the frame of the corresponding Ag_m or Ni_p clusters used as initial geometry was deformed. Finally, we have tried to construct Ag_mNi_p clusters starting from structures obtained for Ag_{m–1}Ni_p and Ag_mNi_{p–1} isomers. Of course, the explicit treatment of all the electrons in a cluster having a large number of atoms constitutes a demanding computational task, and the search for the lowest isomer cannot include a global optimization procedure of the potential energy surface. So we cannot be sure that a more stable cluster than those found in our calculations does not exist. Harmonic frequency analysis was performed to verify that the optimized structures are local minima. As nickel is a magnetic metal, several spin multiplicities for each structure were tested. In the Discussion we report only on the lowest-energy stable isomers determined in our optimizations. For each stable structure, the

charge and local spin density on atoms have been estimated through a natural population analysis (NPA).^{29,30}

3. Results and Discussion

A. Structural Properties and Cohesive Energies. The optimized geometries of the lowest energy isomers of Ag_mNi_p clusters ($m + p \leq 6$) are shown in Figure 1, together with the spin multiplicities and spatial symmetries. We do not report all the optimized structures here, but coordinates of isomers are available upon request. For the monometallic Ag_m and Ni_p clusters, we have found the same geometries as those described in previous works, that is, planar structures^{3,24,25,31–34} for Ag_m (an obtuse triangle for Ag₃, a rhombus for Ag₄, a trapezoid for Ag₅, and a planar D_{3h} triangle for Ag₆) and three-dimensional compact structures^{35,36} for Ni_p (an acute triangle for Ni₃, a compact tetrahedron for Ni₄, a triangular bipyramid for Ni₅, and a square bipyramid for Ni₆). Contrary to Ag, Ni atoms show clearly a tendency to get the highest coordination, maximizing the number of Ni–Ni bonds. As explained in the following, the structure of the Ag_mNi_p clusters is determined by this difference of Ag and Ni atoms behavior.

The shape of Ag₂Ni is a quasi-equilateral triangle with an apex angle of 60.2°, while that of AgNi₂ is an acute isosceles triangle with an apex angle of 52.8°. The structure of Ag₃Ni, Ag₂Ni₂, and AgNi₃ is a rhombus, analogous to that of Ag₄ but different from that of Ni₄. As for Ag₅, the geometry of both Ag₄Ni and Ag₃Ni₂ is a trapezoid, while both Ag₂Ni₃ and AgNi₄ are triangular bipyramids like Ni₅. In Ag₂Ni₃ the two Ag atoms are located on both sides of a triangle Ni₃. Both Ag₄Ni₂ and Ag₃Ni₃ have a triangular structure similar to that of Ag₆ in which the inner sites are occupied by Ni atoms. Ag₅Ni presents a

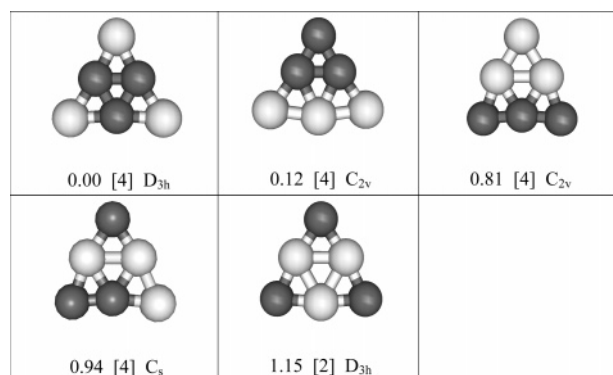


Figure 2. Stable triangular structures found for Ag_3Ni_3 . Relative energies (in electronvolts), spin multiplicities (in brackets), and spatial symmetries are given.

pentagonal structure with the Ni atom surrounded by the five silver atoms, similar to the structure found by Hou et al.¹⁸ In the $\text{Ag}_{6-p}\text{Ni}_p$ series, the two- or three-dimensional structure depends on the number of nickel atoms: if p is less than 4, the cluster is flat; otherwise it corresponds to a compact three-dimensional structure. So planar structures seem to be favored as the number of Ag atoms is at least equal to that of Ni atoms, while three-dimensional structures correspond to clusters with more Ni atoms than Ag atoms.

Moreover, it can be observed that the Ni atoms tend to be gathered together. In all the Ag_mNi_p clusters, for $p \geq 2$, the nickel atoms are brought together, yielding a maximum of Ni–Ni bonds, and the silver atoms seem to be located around a Ni core with a maximum of Ag–Ni bonds. In order to illustrate this property, we have plotted in Figure 2 stable triangular Ag_3Ni_3 structures. It appears clearly that the three Ni atoms favor structures with three Ni–Ni bonds, silver atoms being scattered around a Ni_3 core with two Ag–Ni bonds for each Ag atom. Likewise, the pentagonal Ag_5Ni , maximizes the number of Ag–Ni bonds. This structure is 0.17 eV below the triangular structure in which the Ni atom is located on a side. The triangular structure with the Ni atom on a corner is 0.46 eV above the lowest-energy isomer. Let us note that other three-dimensional structures, not shown in Figure 2, with a Ni_3 core are found to be lower than some triangular structures plotted here. For large Ag–Ni clusters, previous works^{4–7,10} have demonstrated that the tendency for Ag to segregate toward the cluster surface was due to (i) the stronger Ni–Ni bonds as compared to the Ag–Ag ones and (ii) the larger Ag atomic radius. The first argument is also valid for the small clusters studied here, but the second one is not. The clusters studied in this work are too small to account for the respective positions of Ni and Ag from the bond lengths since all the atoms are located at the surface. For example, for Ag_3Ni_3 the substitution of the three Ni in the inner sites by the three Ag does not significantly deform the structure and does not considerably modify the bond lengths.

Finally, it can be inferred that, in most of the Ag_mNi_p clusters, the structure can be built from the stablest $\text{Ag}_{m-1}\text{Ni}_p$ by adding one Ag atom. For example, the structure of Ag_4Ni is obtained from Ag_3Ni by adding one Ag atom, connected to Ni. Similarly, Ag_3Ni_2 is built from Ag_2Ni_2 with a silver atom added to the rhombus. Nevertheless, this rule of growth is not absolute since the two- or three-dimensional geometry is also handled by the Ag/Ni ratio.

The spin multiplicity of the lowest energy isomer is also given in Figure 1. Several multiplicities have been tested for each structure, but the excited multiplets are found to be very much

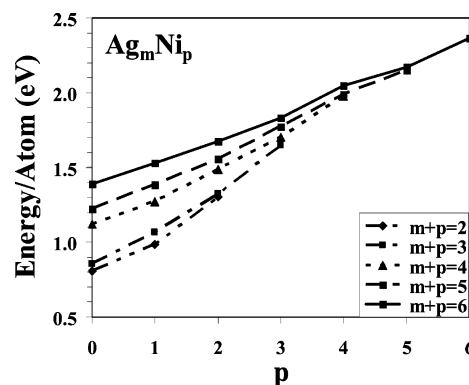


Figure 3. Cohesive energies of Ag_mNi_p clusters as a function of p for fixed $m + p$ values.

TABLE 1: Spin Multiplicities ($2S + 1$) of Ag_mNi_p Clusters^a

p	$m + p = 3$	$m + p = 4$	$m + p = 5$	$m + p = 6$
1	3	2	3	2
2	2	3	2	3
3	3	4	3	4
4		5	4	5
5			7	6
6				9

^a Shown in italic type are spin multiplicities of bare Ni_p .

higher than the ground state. For example, the doublet is found to be 0.66 eV above the quartet for Ag_3Ni_3 , while the quintet for Ag_2Ni_3 is found to be 0.70 eV above the triplet. For Ag_mNi_p , the multiplicity increases monotonically with the number of Ni atoms but never exceeds that of Ni_p clusters (Table 1). For a given number of Ni atoms, the multiplicities change only by one unit as the number of silver atoms varies. As expected from the magnetic behavior of nickel, the spin multiplicity depends only on the number of nickel atoms, and silver atoms have little influence.

The cohesive energies defined as $E_c = -[E(\text{Ag}_m\text{Ni}_p) - mE(\text{Ag}) - pE(\text{Ni})]/(m + p)$ are plotted in Figure 3 as a function of p for the fixed total number of atoms $m + p = 2, 3, 4, 5$, and 6. The calculations yield a monotonic increase, indicating that for a given value of $m + p$ the substitution of one Ag atom by one Ni atom in the Ag_mNi_p cluster always brings a positive quantity of energy. Moreover, the slope decreases slightly with the increase of the total number of atoms $m + p$. This means that the Ag–Ni substitution corresponds to a lower increase in cohesive energy as the size grows. So the effect of the substitution is less important in a large cluster than in a small one. The mean value of the increase of the cohesive energy is about 0.2 eV by substituted atom. Let us note that, unexpectedly, adding a first Ag atom to a pure Ni_p cluster does not significantly enhance the cohesive energy per atom.

B. Electronic Properties. Vertical ionization potentials (IP_v) have been calculated for each Ag_mNi_p cluster. The results are shown in Figure 4 as a function of the total number of atoms. The spin multiplicities of the positively charged clusters are given in Figure 1. Figure 4a gives the evolution of IP_v for clusters with a low number of Ni atoms ($p \leq 2$). The $p = 0$ curve corresponds to Ag_m clusters, for which the IP_v shows an even–odd alternation as m increases. In this case, a very good agreement with the available experimental data³⁷ is found. For the Ag_mNi and Ag_mNi_2 clusters, the IP_v behavior is close to that of Ag_m . This is correlated with the fact these clusters and Ag_m clusters of the same size have the same geometry (Figure 1). In Figure 4b, we have represented the evolution of IP_v for cluster with the number of Ni atoms $p = 3, 4$, or 5. The IP_v

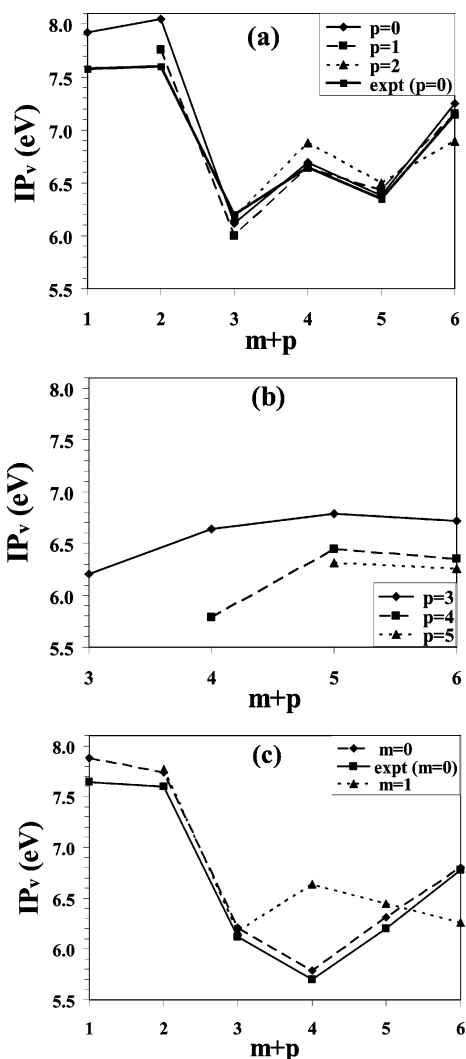


Figure 4. Calculated vertical ionization potentials for Ag_mNi_p clusters. Experimental data for Ag_m are taken from ref 37, while those for Ni_p are from ref 38.

curves are then more regular, without alternation, and seem to reach an asymptotic value for $p = 3$ or 4. Let us notice, too, that IP_v decreases as the number of Ni atoms increases for a given total size of the cluster. The behavior is then quite different from the previous cases, and so we have two classes of clusters, depending on the p value. In each case, the evolution of IP_v needs an interpretation from the knowledge of the electronic structure. In Figure 4c, IP_v is plotted as a function of the total number of atoms $m + p$, for two different values of the number of Ag atoms, $m = 0$ or 1. Of course $m = 0$ corresponds to the pure Ni clusters, and a comparison with experiment³⁸ is shown in Figure 4c. For Ni_p clusters the curve presents a minimum for $p = 4$, which is in very good accord with experiment. In AgNi_p clusters ($m = 1$ curve in Figure 4c), the values for AgNi_3 and AgNi_5 differ from those of the pure Ni cluster of the same size; this can be associated with a noticeably different geometry (Figure 1).

To further understand the link of IP_v and the electronic structure of the clusters, we have plotted the highest occupied molecular orbital (HOMO) for neutral clusters. The HOMO of $\text{Ag}_{6-p}\text{Ni}_p$ are given in Figure 5. For small values of p , it appears clearly that the HOMO is similar to that of Ag_6 and is located essentially on Ag atoms, independently of the Ag/Ni composition. The previous analysis can be generalized to all sizes $n + p$ with small p and explains the fact that the IP_v of mixed

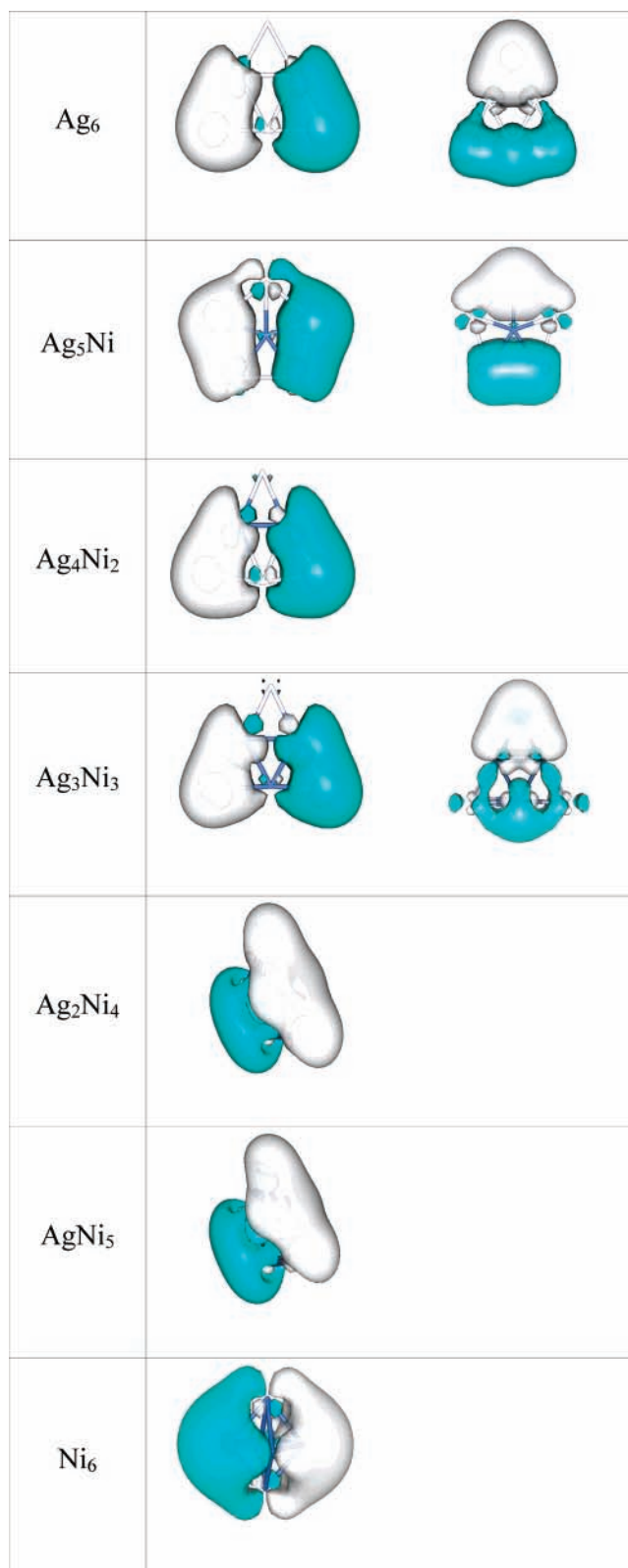


Figure 5. HOMO for $\text{Ag}_{6-p}\text{Ni}_p$ clusters. Isovalue is 0.02 au. The doubly degenerate HOMOs are represented on the same line. The HOMO for Ni_6 is triply degenerate along the three axes, but only one component is shown.

Ag_mNi_p is similar to that of Ag_m (Figure 4a), since both the geometrical structure and the HOMO are similar. Upon increasing the number of Ni atoms, the cluster becomes three-dimensional and the HOMO is delocalized on the whole cluster. However, AgNi_5 and Ni_6 do not have exactly the same HOMO

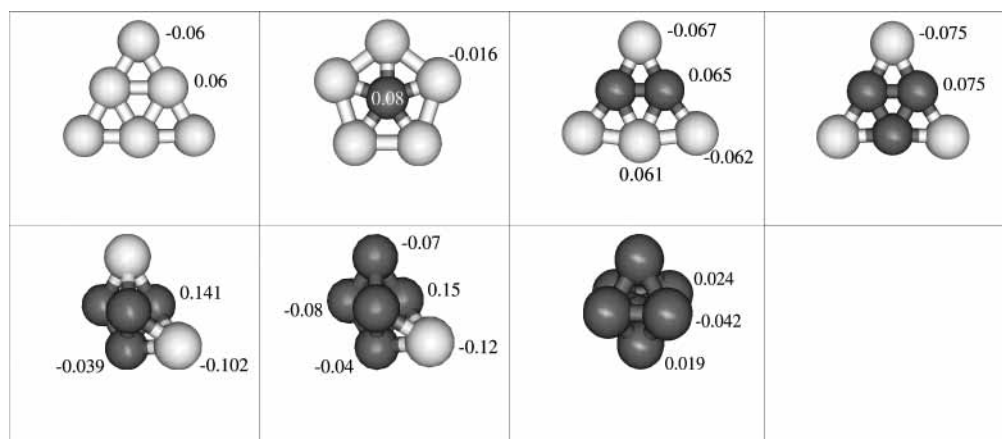


Figure 6. Atomic charges (in atomic units) from the natural population analysis for $\text{Ag}_{6-p}\text{Ni}_p$ clusters.

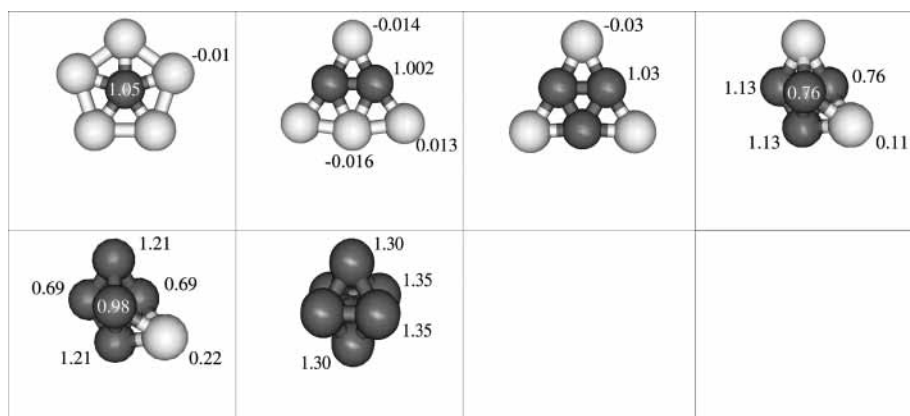


Figure 7. Local atomic spin densities from the natural population analysis for $\text{Ag}_{6-p}\text{Ni}_p$ clusters.

because of the difference in their geometry, and so their IP_v values differ.

To further understand the interaction between Ni and Ag atoms, natural population analysis (NPA) was performed. The calculated charges on silver and nickel atoms in $\text{Ag}_{6-p}\text{Ni}_p$ are given in Figure 6. A very low electronic charge transfer from Ni to Ag can be noted. From this outlook, no specificity of the Ag–Ni, Ag–Ag, or Ni–Ni bonds is evidenced. The charge transfer from Ni to Ag is almost the same as that from inner Ag to outer Ag (0.075 in Ag_3Ni_3 compared to 0.060 in Ag_6). A positive charge is found on inner atoms while a negative charge is found on atoms placed outside. This behavior is usual for surface atoms with a low coordination number, when the atomic layer is more than half-full. The electronic configurations obtained from the natural population analysis show that the configurations of Ag atom remain close to that in the atomic situation, that is, $4d^{10}5s^1$, while that for Ni is close to $3d^94s^1$. For example, the natural electron configuration in Ag_3Ni_3 is $5s^{1.14}d^{9.95}5p^{0.02}6p^{0.01}$ on Ag and $4s^{0.95}3d^{8.90}4p^{0.07}$ on Ni.

We have also calculated the local atomic spin densities from the natural population analysis as the difference between the occupation numbers in spin-up and spin-down states. The magnetic moment is found to be localized on the nickel atoms with very little contribution from silver atoms when the number of Ag atoms predominates (Figure 7). Nevertheless, a spin polarization on silver atoms appears when the number of Ag atoms decreases. The local magnetic moment found here on Ni atoms is in good agreement with that of Sun et al.³⁹ on Ag_{12}Ni cluster resulting from a Mulliken population analysis.

4. Conclusion

The structure and electronic properties of small Ag_mNi_p clusters ($m + p \leq 6$) have been investigated, in order to elucidate the relative specificity of the two metals. The two- or three-dimensional geometry of the clusters is determined by the ratio between the number of Ni and Ag atoms. When the number of Ni atoms is less than the number of Ag atoms, the cluster is flat; otherwise it has a three-dimensional geometry. In the most stable structures, the Ni atoms occupy the highest coordinated sites and they tend to be gathered, setting a Ni core, with outer Ag atoms. This configuration prefigures the core–shell shape of large bimetallic nanoclusters. When the electronic properties are considered, the vertical ionization potential and the highest occupied molecular orbital shape are directly related to the geometry of the cluster. The two-dimensional clusters have electronic properties dominated by the Ag contributions, whereas for three-dimensional geometries, these properties depend on both Ag and Ni atoms. This is clearly demonstrated by the expansion of the HOMO on the whole cluster. The charge transfer between the atoms in the clusters remains very low, pointing out no specificity of the bond between Ag and Ni atoms. The behavior of these small clusters is expected to be a good model of the structural properties of larger Ag–Ni systems. It will be a guide for the understanding of the electronic properties of a series of 13-atom AgNi clusters, which will be described in a future paper.

Acknowledgment. The authors thank the Centre Informatique National de l'Enseignement Supérieur (CINES) at Montpellier, France, for generous allocation of computation time under Contract No. c20060822452.

References and Notes

- (1) Jellinek, J.; Krissinel, E. B. In *Theory of Atomic and Molecular Clusters*; Jellinek, J., Ed.; Springer: Berlin, Germany, 1999; pp 277–308.
- (2) Derosa, P. A.; Seminario, J. M.; Balbuena, P. B. *J. Phys. Chem. A* **2001**, *105*, 7917.
- (3) Lee, H. M.; Ge, M.; Sahu, B. R.; Tarakeshwar, P.; Kim, K. S. *J. Phys. Chem B* **2003**, *107*, 9994–10005.
- (4) Rossi, G.; Rapallo, A.; Mottet, C.; Fortunelli, A.; Baletto, F.; Ferrando, R. *Phys. Rev. Lett.* **2004**, *93*, 105503.
- (5) Baletto, F.; Mottet, C.; Rapallo, A.; Rossi, G.; Ferrando, R. *Surf. Sci.* **2004**, *192–196*, 566–568.
- (6) Rapallo, A.; Rossi, G.; Ferrando, R.; Fortunelli, A.; Curley, B. C.; Lloyd, L. D.; Tarbuck, G. M.; Johnson, R. L. *J. Chem. Phys.* **2005**, *122*, 194308.
- (7) Ferrando, R.; Fortunelli, A.; Rossi, G. *Phys. Rev. B* **2005**, *72*, 085449.
- (8) Portales, H.; Saviot, L.; Duval, E.; Gaudry, M.; Cottancin, E.; Pellarin, M.; Lermé, J.; Broyer, M. *Phys. Rev. B* **2002**, *65*, 165422.
- (9) Moskovits, M.; Srnova-Sloufova, I.; Vickova, B. *J. Chem. Phys.* **2002**, *116*, 10435.
- (10) Gaudry, M.; Cottancin, M.; Pellarin, M.; Lermé, J.; Arnaud, L.; Huntzinger, J. R.; Vialle, J. L.; Broyer, M. *Phys. Rev. B* **2003**, *67*, 155409.
- (11) Sun, S.; Murray, C. B.; Weller, D.; Folks, L.; Moser, A. *Science* **2000**, *287*, 1989.
- (12) Dennler, S.; Ricardo-Chavez, J. L.; Morillo, J.; Pastor, G. M. *Eur. Phys. J. D* **2003**, *24*, 237.
- (13) Janssens, E.; Neukermans, S.; Nguyen, H. M. T.; Nguyen, M. T.; Lievens, P. *Phys. Rev. Lett.* **2005**, *94*, 113401.
- (14) Molenbroek, A. M.; Norskov, J. K.; Clausen, B. S. *J. Phys. Chem. B* **2001**, *105*, 5450.
- (15) Mitric, R.; Burgel, C.; Burda, J.; Bonacic-Koutecky, V.; Fantucci, P. *Eur. Phys. J. D* **2003**, *24*, 41–44.
- (16) Zhao, J. J.; Xie, R. H. *Phys. Rev. B* **2003**, *68*, 035401.
- (17) Zhang, H.; Zelmon, D. E.; Deng, L.; Liu, H. K.; Teo, B. K. *J. Am. Chem. Soc.* **2001**, *123*, 11300.
- (18) Hou, X.-J.; Janssens, E.; Lievens, P.; Nguyen, M. T. *Chem. Phys.* **2006**, *330*, 365–379.
- (19) Frisch, M. J.; Trucks, G. W.; Schlegel, H. B.; Scuseria, G. E.; Robb, M. A.; Cheeseman, J. R.; Zakrzewski, V. G.; Montgomery, J. A., Jr.; Stratmann, R. E.; Burant, J. C.; Dapprich, S.; Millam, J. M.; Daniels, A. D.; Kudin, K. N.; Strain, M. C.; Farkas, O.; Tomasi, J.; Barone, V.; Cossi, M.; Cammi, R.; Mennucci, B.; Pomelli, C.; Adamo, C.; Clifford, S.; Ochterski, J.; Petersson, G. A.; Ayala, P. Y.; Cui, Q.; Morokuma, K.; Malick, D. K.; Rabuck, A. D.; Raghavachari, K.; Foresman, J. B.; Cioslowski, J.; Ortiz, J. V.; Baboul, A. G.; Stefanov, B. B.; Liu, G.; Liashenko, A.; Piskorz, P.; Komaromi, I.; Gomperts, R.; Martin, R. L.; Fox, D. J.; Keith, T.; Al-Laham, M. A.; Peng, C. Y.; Nanayakkara, A.; Gonzalez, C.; Challacombe, M.; Gill, P. M. W.; Johnson, B.; Chen, W.; Wong, M. W.; Andres, J. L.; Head-Gordon, M.; Replogle, E. S.; Pople, J. A. *Gaussian 98*, revision A.6; Gaussian, Inc.: Pittsburgh, PA, 1998.
- (20) Becke, A. D. *Phys. Rev. A* **1988**, *38*, 3098–3100.
- (21) Perdew, J. P. *Phys. Rev. B* **1986**, *33*, 8822–8824.
- (22) Bonacic-Koutecky, V.; Boiron, M.; Pittner, J.; Fantucci, P.; Koutecky, J. *Eur. Phys. J. D* **1999**, *9*, 183–187.
- (23) Rabilloud, F.; Spiegelman, F.; L'Hermite, J. M.; Labastie, P. *J. Chem. Phys.* **2001**, *114*, 289–305.
- (24) Bonacic-Koutecky, V.; Veyret, V.; Mitric, R. *J. Chem. Phys.* **2001**, *115*, 10450–10460.
- (25) Huda, M. N.; Ray, A. K. *Eur. Phys. J. D* **2003**, *22*, 217–227.
- (26) Idrobo, J. C.; Ogut, S.; Jellinek, J. *Phys. Rev. B* **2005**, *72*, 085445.
- (27) Hay, P. J.; Wadt, W. R. *J. Chem. Phys.* **1985**, *82*, 299–310.
- (28) Allouche, A. R. Gabedit is a free graphical user interface for computational chemistry packages. It is available from <http://gabedit.sourceforge.net>.
- (29) Reed, A. E.; Weinhold, F. *J. Chem. Phys.* **1983**, *78*, 4066–4073.
- (30) Reed, A. E.; Weinstock, R. B.; Weinhold, F. *J. Chem. Phys.* **1985**, *83*, 735–746.
- (31) Poteau, R.; Heully, J. L.; Spiegelmann, F. *Z. Phys. D: At., Mol., Clusters* **1997**, *40*, 479–482.
- (32) Fournier, R. *J. Chem. Phys.* **2001**, *115*, 2165–2177.
- (33) Fernandez, E.; Soler, J. M.; Garzon, I. L.; Balbas, L. C. *Phys. Rev. B* **2004**, *70*, 165403.
- (34) Idrobo, J. C.; Ogut, S.; Jellinek, J. *Phys. Rev. B* **2005**, *72*, 085445.
- (35) Reuse, F. A.; Khanna, S. N. *Chem. Phys. Lett.* **1995**, *234*, 77–81.
- (36) Reddy, B. V.; Nayak, S. K.; Khanna, S. N.; Rao, B. K.; Jena, P. *J. Phys. Chem. A* **1998**, *102*, 1748–1759.
- (37) Jackschath, C.; Rabin, I.; Schulze, W. *Z. Phys. D: At., Mol., Clusters* **1992**, *22*, 517.
- (38) Knickelbein, M. B.; Yang, S.; Riley, S. J. *J. Chem. Phys.* **1990**, *93*, 94.
- (39) Sun, Q.; Wang, Q.; Yu, J. Z.; Li, Z. Q.; Wang, J. T.; Kawazoe, Y. *J. Phys. I* **1997**, *7*, 1233.